Elemento de Viga Baseado em Formulação de Rigidez Enriquecido com Funções de Forma Adaptativas para Garantir Equilíbrio Axial

DANILO TARQUINI
Aluno de Doutoramento
EESD Lab, EPFL
Lausanne, Suiça

JOÃO P. ALMEIDA
Investigador de Pós-Dout.
EESD Lab, EPFL
Lausanne, Suiça

KATRIN BEYER
Professora Auxiliar
EESD Lab, EPFL
Lausanne, Suiça

SUMÁRIO

A análise do comportamento inelástico de estruturas, quer ao nível global (força-deslocamento) quer local (tensão-extensão), é fundamental no contexto de avaliações baseadas em critérios de desempenho (*Performance Based Earthquake Engineering*). Tal objectivo é atualmente atingido fazendo uso de ferramentas numéricas que requerem um significativo esforço computacional.
Nomeadamente, elementos de viga baseados em plasticidade distribuída oferecem um bom compromisso entre a precisão de resultados obtida e o tempo de análise requerido, sendo por isso o tipo de elementos finitos mais usualmente utilizado em análises estruturais. Dentro desta categoria, as formulações baseadas em deslocamentos são as mais simples em termos de desenvolvimento analítico e implementação numérica.
No entanto, uma desvantagem fundamental destas últimas relaciona-se com o campo de deslocamentos axiais imposto. Esta limitação implica que o equilíbrio pode apenas ser verificado de uma forma ponderada (i.e., em média) e, quando a não-linearidade material é adicionalmente considerada, tal traduz-se no desenvolvimento de diferentes valores do esforço axial em secções de integração distintas. Consequentemente, a capacidade de flexão do membro estrutural é frequentemente sobrestimada, levando a um desempenho deficiente do elemento finito.
O presente artigo introduz um novo elemento baseado em deslocamentos que verifica o equilíbrio axial de uma forma estrita. Este último foi implementado pelos autores num código de elementos finitos *ad hoc*, e o seu desempenho é mostrado através de dois exemplos de aplicação. Comparações com a formulação clássica de deslocamentos e com a formulação de forças são também mostradas, ao nível local e global.

ABSTRACT

In the framework of Performance Based Earthquake Engineering (PBEE), assessing the inelastic behaviour of structures both at the global (force-displacement) and local (stress-

strain) level is of priority importance. This goal is typically achieved by advanced nonlinear analysis that rely on the use of increasing computational power.
Due to a good compromise between accuracy and processing time, distributed plasticity beam elements represent the most employed finite element in nonlinear structural analysis. In particular, displacement-based elements are the simplest in terms of implementation and the most efficient from the state determination viewpoint.
However, a fundamental drawback of classical displacement-based formulations is related to the assigned axial displacement field. This limitation implies that equilibrium is only verified on an average sense and, in case of material nonlinearity, it yields different values of the axial force in distinct integration sections. This results in a misevaluation of the moment capacity of the structural member and therefore in a poor local and global performance of the finite element.
In this paper a new displacement-based element strictly verifying the axial equilibrium condition is introduced. The latter was implemented by the authors in an *ad hoc* finite element software and its performance is presented by means of two application examples. Comparisons between classical displacement-based and force-based formulations are made, both at the global and local level.

PALAVRAS-CHAVE: Elementos viga, Equilíbrio axial, Formulação de deslocamentos, Formulação de forças, Discretização por fibras.

1. INTRODUCTION

In the framework of Performance Based Earthquake Engineering (PBEE), a reliable assessment of the inelastic behaviour of structures is of fundamental importance. Nonlinear analysis provides the means for calculating the structural response beyond the elastic range and assessing the expected level of damage, following which a decision on whether or not retrofit measures are required should be taken.
One of the most commonly employed tool for the simulation of the nonlinear response of reinforced concrete (RC) structures is represented by beam element models, as they feature an attractive compromise between accuracy and computational cost. Amongst beam formulations, lumped and distributed plasticity approaches can be distinguished. The former, as the name suggests, concentrate the occurrence of inelastic deformations in pre-defined locations along the element length. On the other hand, distributed plasticity elements do not impose *a priori* a specific location for the development of plasticity nor restraints to its progression along the member length. Such type of formulations discretize the element into several numerical integration sections from which the response is obtained. Each section is typically subdivided into fibres to which an inelastic material constitutive law is assigned.
Within distributed plasticity elements, the choice of the imposed independent fields yields the so-called displacement-based (DB) and force-based (FB) formulations [1]. An important point, in the context of the present work and as further discussed below, is that most of these approaches have been developed for Euler-Bernoulli beam theory (plane sections remain plane and perpendicular to the deformed element axis), which is the form that is available in roughly all the commonly used structural analysis software (e.g., [2,3]). DB formulations employ linear and Hermitian polynomial functions for the axial and transversal displacement fields respectively (which provides an exact solution only for the case of linear elastic material and nodal loads). FB formulations, on the other hand, use constant and linear shape functions for the axial force and bending moment respectively (which gives an exact solution regardless of the material nonlinearity assigned to the fibres). Therefore, one FB element usually suffices to simulate the nonlinear response of a structural member while if DB elements are used member discretization in several finite elements is required. Additionally, and importantly for the purpose of the present work, equilibrium in FB formulations is verified pointwise along the element length whereas in DB elements only the average of the internal forces is in equilibrium with the nodal forces (i.e., equilibrium is only verified in an average sense).

Despite the undebatable superiority of FB elements over the DB counterpart in terms of theoretical accuracy, DB elements are more straightforward and less computationally burdensome for what concerns their formulation and numerical implementation in a Finite Element code.

In the present work it is postulated that DB formulations, which have been gradually replaced by FB approaches over the past 15-20 years, have good reasons to be revived as they offer a bypass around some of the limitations that stem from the application of the well-known Euler-Bernoulli hypothesis. In fact, the latter has been shown experimentally to be quite constraining. As pointed out by Priestley et al. [4], the first reason for the mismatch between the force-displacement response as obtained from a FB element (which verifies equilibrium in an exact form) and experimental results is the fact that tension shift effects are ignored. The latter cause a linear distribution of plastic curvatures inside the plastic zone of the structural member ([5–8], see Figure 1). Furthermore, a recent test campaign on circular bridge piers [8] has shown that the intersection of this plastic curvature profile with the elastic curvatures occurs at an increasing height for larger ductility demands (see again Figure 1). The two above physical phenomena can be analytically simulated by imposing appropriate lateral displacement profiles (in accordance with the observed curvatures), suggesting that DB approaches (and not FB formulations) are the natural framework to develop such finite element. This paper is a first step to address these issues and hence to gradually reflect unanimous experimental findings in beam elements that can later be used more confidently in engineering practice.

To accomplish such goal, one fundamental drawback of the classical DB formulations should be addressed beforehand. The imposed axial displacement field implies that equilibrium is only verified on an average sense which, in case of material nonlinearity, results in different values of the axial force for distinct integration sections. This leads to a misevaluation of the moment capacity of the structural member and therefore to a poor local and global performance of the finite element. This paper presents an enhanced DB element in which the axial equilibrium is strictly verified (hence somehow emulating the advantages of a FB formulation) through the use of adaptive shape functions for the generalized strains. This formulation will be further extended in the future to include transversal displacement profiles that simulate the above mentioned effect of tension shift.

The new element and its state determination are described in Section 2. Section 3 presents two application examples showing the comparison between the new element and the classical DB and FB formulations, whilst future developments and conclusions are provided in Section 4.

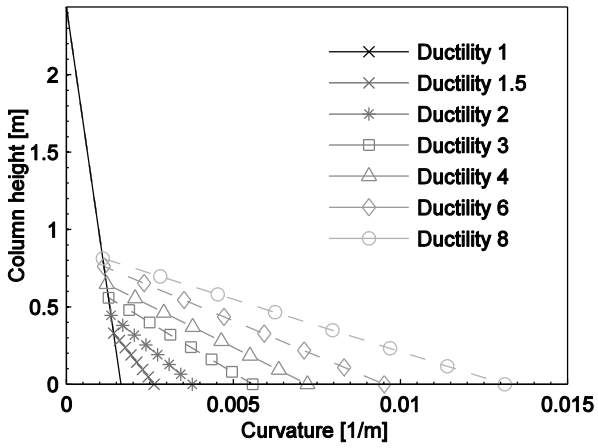

Figure 1: Measured curvature profile in a circular cantilever pier for different levels of imposed displacement ductility (adapted from [8]).

2. AXIALLY EQUILIBRATED DISPLACEMENT-BASED ELEMENT: STATE DETERMINATION

The state determination of the enhanced displacement-based element satisfying axial equilibrium is schematically illustrated in the flowchart of Figure 2(a). It consists in determining the element basic forces and tangent stiffness matrix given a set of incremental basic displacements. The element forces P_{bas} and displacements U_{bas} acting on the element in the basic reference system (e.g. without rigid body modes) are shown in Figure 2(b). They include the nodal axial force/bending moments (P_1, M_1, M_2) and the end axial displacement/rotations (U_1, θ_1, θ_2). The steps to be performed to go from the basic to the global reference systems involve classical structural analysis operations (e.g. the use of rotation matrix and nonlinear compatibility and equilibrium relations, such as those associated to a corotational formulation) and will thus be omitted.

In the classical DB formulations, a linear shape function for the axial displacement field $u(x)$—i.e. corresponding to a constant average axial strain profile $\varepsilon_0(x)$—is employed along the element. Hermitian polynomials are used instead for the transverse displacement field $v(x)$ resulting in a linear curvature profile $\kappa(x)$. When nonlinear material behaviour is considered, such generalized deformations lead to internal generalized forces—$N(x)$, $M(x)$—which are not strictly equilibrated, but only on an average sense.

Straightforward equilibrium considerations imply that, when no distributed axial loads are applied along the element axis, the axial force $N(x)$ has to be the same in all integration sections and equal to the basic axial force P_1. The former condition, combined with the fact that the integral (along the element length) of the average axial strain $\varepsilon_0(x)$ must be equal to the applied axial displacement U_1, can be manipulated to provide direct relationships between $\Delta\varepsilon_0(x_i)$ and the current generalized axial force $N(x_i)$ at each integration point (IP) i [9]. An iterative procedure that systematically adjusts the values of the incremental axial strains $\Delta\varepsilon_0(x_i)$ can therefore be set up until the difference between the generalized axial forces $N(x_i)$ in all the integration sections is below a defined tolerance [9]. Once convergence is attained, the set of axial strains $\varepsilon_0(x_i)$ strictly satisfying axial equilibrium is known and the generalized strains' shape functions can be updated. The principle of virtual work is then applied in order to determine the set of equilibrated element basic forces as well as a consistent element tangent basic stiffness matrix K_T.

3. APPLICATION EXAMPLES

The axially equilibrated displacement-based formulation has been implemented in the finite element software *SAGRES* (*Software for Analysis of GRadient Effects in Structures*), originally developed by the second author. In the following subsections, two application examples compare the accuracy of the proposed formulation with respect to the classical displacement-based and force-based approaches. The influence of the constant axial force criterion will be examined in detail as well as the need for member discretization into several finite elements.

In both application examples, the reference structure is represented by a 3 m height cantilever column, to which an external constant axial load P and an incremental lateral displacement Δ are applied.

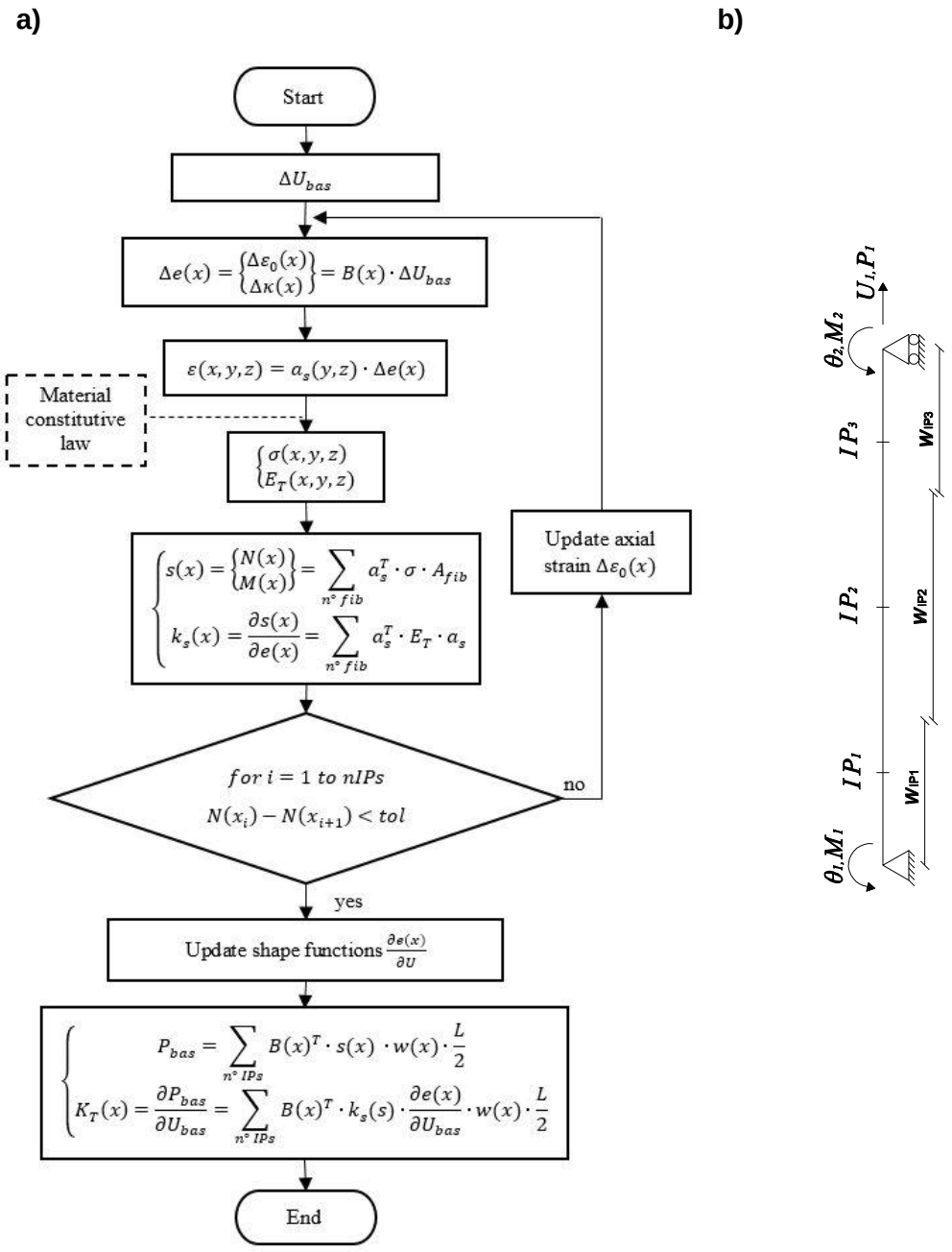

Figure 2: (a) Procedure for the element state determination; (b) Element basic forces and displacements.

3.1. Steel column

A steel column is considered in this first application example. The column section (roughly corresponding to an HEA 400 profile) is depicted in Figure 3(a) as well as the adopted bilinear material constitutive law—Figure 3(b). The main material properties (which also includes the concrete properties used in the second application example) are listed in Table 1. A coarse sectional discretization and a monotonically increasing steel stress-strain law were chosen, on the one hand to maintain the computational problem as simple as possible, and on the other to avoid numerical problems (such as localization) that may arise with softening behaving materials (e.g. concrete). A high axial

load (3500 kN) was applied with the intention of better contrasting the results obtained through the different beam element formulations employed.

Force-based (FB), classical displacement-based (DB/c), and axially equilibrated displacement-based (DB/ae) elements are used for the simulation of the member inelastic response. In the Figure 4(a) the results obtained with a single beam element to represent the column are displayed. DB elements featured two Gauss-Legendre integration sections while nine Gauss-Lobatto integration points were used for the FB element model. As discussed in Calabrese et al. [10], FB elements are sensitive to the element discretization and a minimum number of 4 IPs is generally required for good-accuracy solutions. DB element models, on the other hand, are only sensitive to the structural discretization and hence it is not justifiable to use more than 2 integration poins per element.

The DB/c element model shows, as expected, a stronger and stiffer response due to the constraints imposed in both the axial and lateral displacement fields. By removing the constraint on the axial displacement field through the iterative procedure introduced in Section 2, the DB/ae becomes considerably softer, yielding a reduction in the simulated lateral strength. However, it can be noted that the latter is still overestimated when compared with the solution provided by the FB formulation, where no displacement fields are assigned and exact equilibrium is satisfied. Multiple DB elements are required to output a force-displacement response closer to that given by the FB model. This is shown in Figure 4(b), where results from models employing 1, 2 and 4 DB elements are displayed. Even though mesh refinement leads both DB approaches to the FB solution, it is evident that the DB/ae element model converges much faster than the one using classical displacement shape functions. Indeed, two DB/ae elements provide a sufficiently accurate solution, which can only be reached with four DB/c.

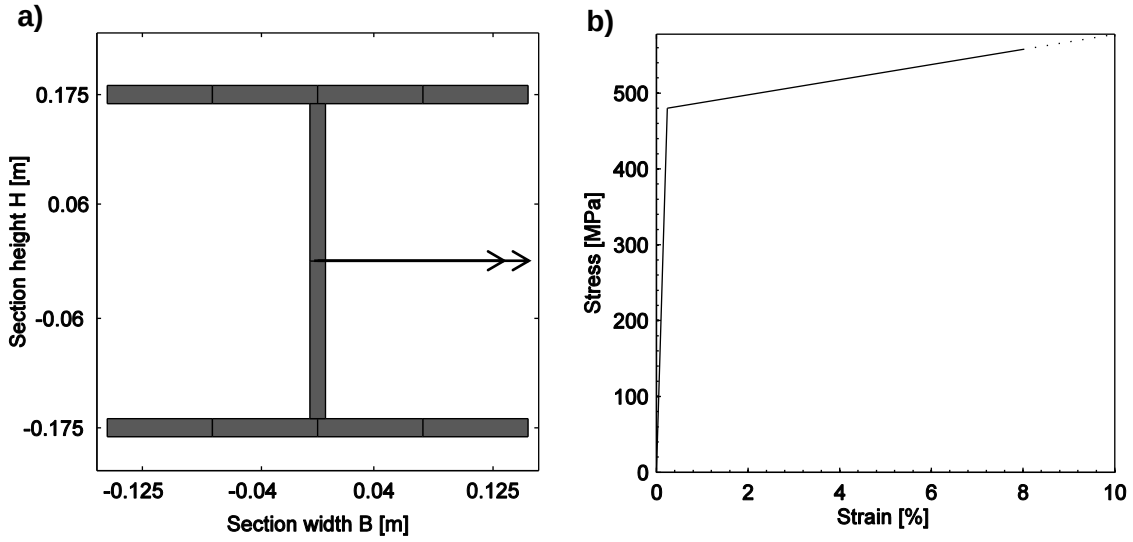

Figure 3: Steel column fibre section: (a) Sectional discretization; (b) Steel stress-strain law.

Table 1 - Main material properties

Reinforcing steel				
f_y [MPa]		E_s [MPa]		b [-]
480		200000		0.005
Concrete				
f_c [MPa]	f_{cc} [MPa]	E_c [MPa]	ε_c [-]	ε_{cc} [-]
37	42	30000	0.002	0.003

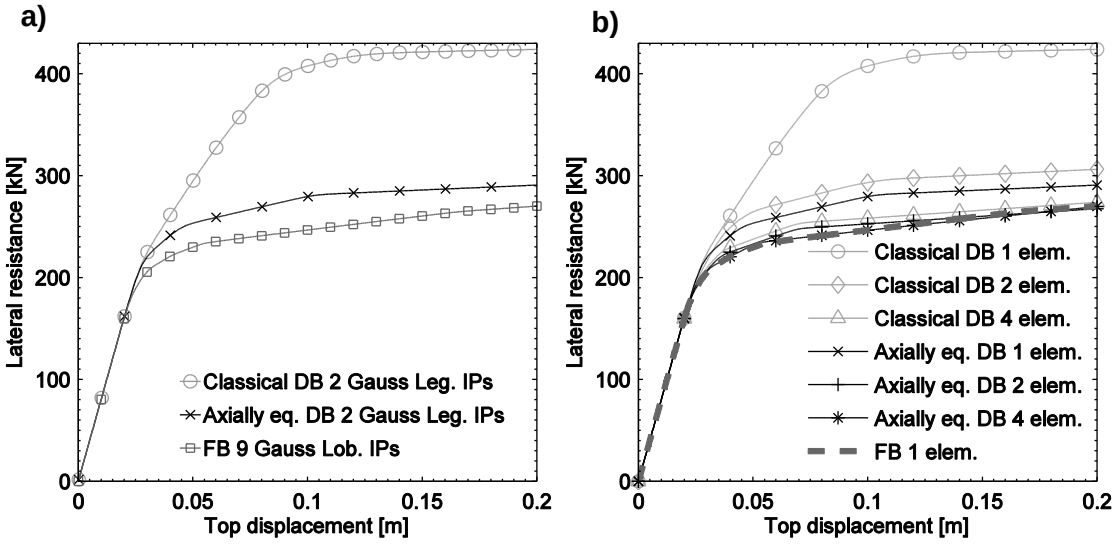

Figure 4: Force-displacement response of the steel column: (a) using one element per member; (b) influence of structural member discretization.

The evolution of the axial force during the analyses is shown in Figure 5(a) for the two integration sections in both the DB/c and DB/ae formulations (case where the structural member was discretized with one finite element only). As it can be observed, after an initial elastic phase (which ends at around load step 150), the linear axial displacement shape function used in the DB/c element leads to different axial force values in the two integration points. Although the average element equilibrium is conserved (the axial forces in the two IPs are symmetric around the value of the imposed axial load), the moment in the two IPs (after inelasticity commences) is computed with values of the axial force that are based on the incorrect assumption of a linear axial displacement distribution along the element length. This inevitably results in a wrong evaluation of the moment capacity for the structural member (which is also due to the inadequate assumption of linear variation of curvatures), and therefore of its lateral resistance. On the contrary, the axial force in both IPs of the DB/ae is constant (i.e., axial equilibrium is strictly verified) and always equal to the external applied axial load, thus providing a better estimate of the element moment capacity. Additionally, Figure 5(b) displays the very good performance of the iterative procedure in terms of the number of global Newton-Raphson iterations required to achieve convergence.

3.2. Reinforced concrete column

A reinforced concrete column represents the case study for the second application example. The section discretization and the employed concrete stress-strain curves are shown respectively in Figure 6(a) and (b). The RC section is 30 cm large and 40 cm deep with 2 cm cover concrete in both directions. The longitudinal reinforcement is composed by 16 steel bars, each one of 10 mm diameter. The mathematical model for both the confined and unconfined concrete is the one proposed by Popovics [11] while the same bilinear constitutive law presented in the previous section—Figure 3(b)—is used for the reinforcing steel. A summary of the main materials properties is given in Table 1.
The global force-displacement responses of FB, DB/c and DB/ae element models are compared in Figure 7. As in the previous section, nine Gauss-Lobatto IPs and two Gauss-Legendre IPs are employed for FB and DB elements respectively. Only one element is used to discretize the structural member and the axial load ratio (ALR) is varied between 1% and 8%. For the same axial load level, the strongest and stiffest response is again provided by the DB/c element models, followed by the DB/ae and the FB ones. The difference between the maximum lateral strength attained by the diffent models for distinct axial load ratios increases with the applied axial load. Taking the

response of the FB model as reference, the average relative error of the DB/c model is around 80% (75%, 80% and 84% for 1%, 4% and 8% ALR respectively) while it reduces to 20% if DB/ae elements are considered (14%, 20% and 26% for 1%, 4% and 8% ALR respectively).
Finally, in Figure 8 the axial strain profiles for the DB/c and DB/ae (ALR=4%) are shown for different levels of drift. Due to the imposed linear axial displacement field, the axial strain profile for the DB/c is constant. As expected, due to the shifting of the neutral axis, positive strain values (tension) increasing with the drift demand are observed. On the other hand, the DB/ae shows different strain values in the distinct integration sections, which are the result of the iterative procedure to obtain a constant axial force along the column. Highest tensile strains are always recorded at the bottom IP. This behaviour is certainly much closer to the reality than the one simulated by the DB/c since the shifting of the neutral axis (caused by the section decompression) occurs at the base of the column, where the moment is maximum, rather than along its entire height.

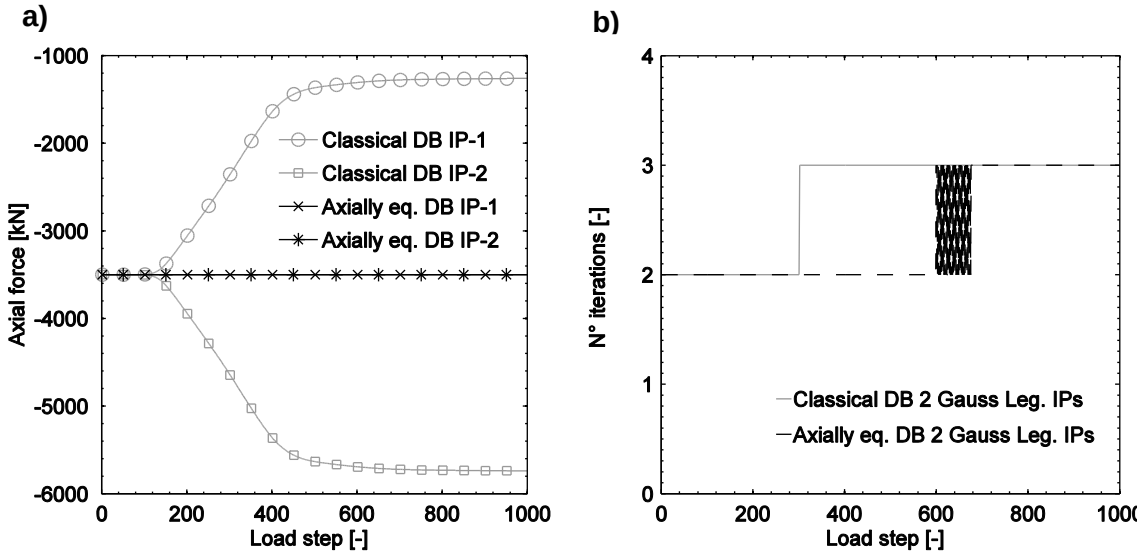

Figure 5: (a) Axial force evolution; (b) Number of Newton-Raphson iterations per load step.

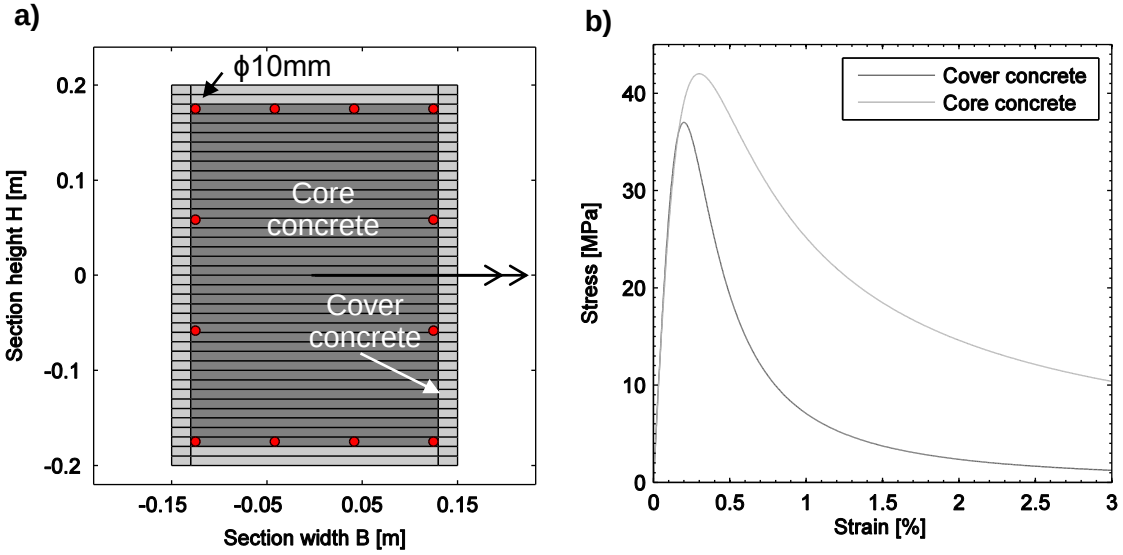

Figure 6: (a) Sectional discretization of the RC column; (b) Uniaxial concrete stress-strain law.

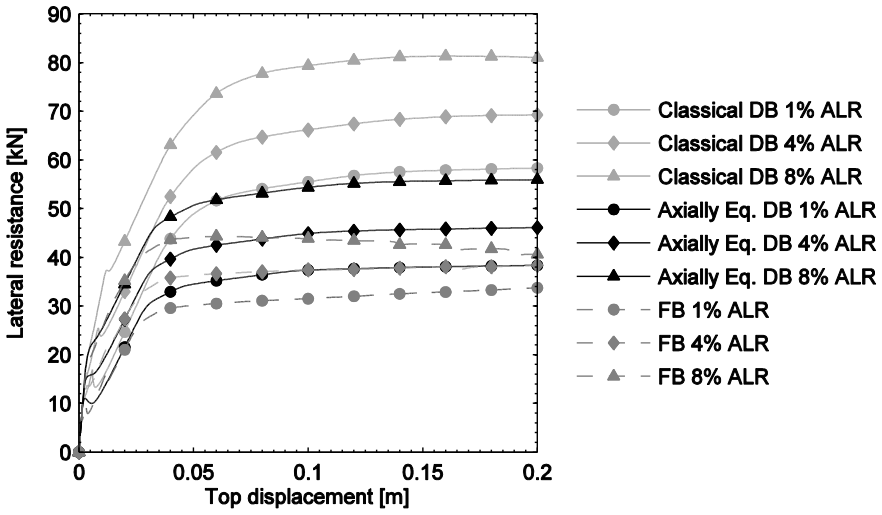

Figure 7: Force-displacement response of the RC column for different axial load ratios.

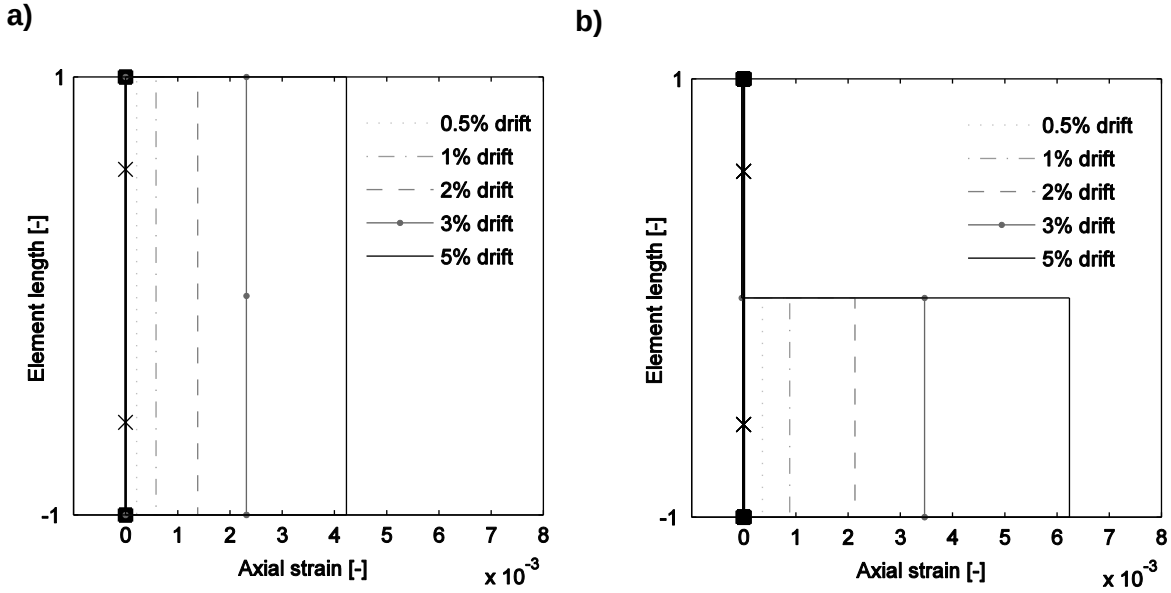

Figure 8: Axial strain profiles at different levels of drift: (a) Classical DB element; (b) Axially equilibrated DB element.

4. CONCLUSIONS AND FUTURE WORK

The linear shape functions used to describe the axial displacement field in a classical displacement-based element constitutes a significant limitation in the accuracy of this finite element formulation when inelastic material behaviour is considered. The resulting axial forces become equilibrated only in an average sense, inevitably leading to a poor local and global performance of the finite element.

In this paper a displacement-based element strictly satisfying axial equilibrium is presented. The pointwise equilibrium is achieved by an intra-element iterative procedure which automatically recalculates the correct axial strain profile required to guarantee such axial force equilibrium. Once the latter condition is met, the principle of virtual work is employed to compute the element basic forces and to obtain a consistent stiffness matrix.

Two application examples are used to compare the element formulation described above against classical displacement-based and force-based approaches. The strengths and weaknesses of the proposed formulation are pinpointed both at the global and local level. Namely, it is shown that when compared to the classical displacement-based approach, a greater accuracy can be obtained in terms of force-displacement response and generalized axial stress-axial strain profiles. The improved predictions do not require relevant additional computational time.
The axially equilibrated DB element presented herein is intended as a first step in the formulation of a more sophisticated beam element. The latter will include the additional modification of the imposed transversal displacement profile in order to account for physically relevant effects in the nonlinear cyclic response of members, such as tension shift, which current beam element models are not able to capture.

5. ACKNOWLEDGMENTS

The financial support provided by the Office fédéral des routes (OFROU) is kindly appreciated.

6. REFERENCES

[1] J.P. Almeida, D. Tarquini, K. Beyer, Modelling approaches for inelastic behaviour of RC walls: Multi-level assessment and dependability of results, Arch. Comput. Methods Eng. 23 (2016) 69–100.
[2] SeismoSoft, SeismoStruct - A Computer Program for Static and Dynamic Nonlinear Analysis of Framed Structures, (2013).
[3] F. McKenna, G.L. Fenves, M.H. Scott, B. Jeremic, Open System for Earthquake Engineering Simulation (OpenSees), Berkeley, California, U.S.A., 2000.
[4] M.J.N. Priestley, G.M. Calvi, M.J. Kowalsky, Displacement-based seismic design of structures, IUSS Press, 2007.
[5] E.M. Hines, Seismic Performance of Hollow Rectangular Reinforced Concrete Bridge Piers with Confined Corner Elements, 2002.
[6] Y.D. Hose, F. Seible, M.J.N. Priestley, Strategic Relocation of Plastic Hinges in Bridge Columns, San Diego, California, 1997.
[7] Y.H. Chai, M.J.N. Priestley, F. Seible, Flexural retrofit of circular reinforced concrete bridge columns by steel jacketing: experimental studies, Struct. Syst. Res. Proj. 91/06, Univ. Calif. (1991) 151.
[8] J.C. Goodnight, M.J. Kowalsky, J.M. Nau, A new look at strain limits and plastic hinge lengths for reinforced concrete bridge columns, in: 10th U.S. Natl. Conf. Earthq. Eng., Anchorage, 2014.
[9] B. Izzuddin, C. Karayannis, A. Elnashai, Advanced nonlinear formulation for reinforced concrete beam-columns, J. Struct. Eng. 120 (1994) 2913–2934.
[10] A. Calabrese, J.P. Almeida, R. Pinho, Numerical issues in distributed inelasticity modeling of RC frame elements for seismic analysis, J. Earthq. Eng. 14 (2010) 38–68. doi:10.1080/13632469.2010.495681.
[11] S. Popovics, A numerical approach to the complete stress-strain curve of concrete, Cem. Concr. Res. 3 (1973) 583–599. doi:10.1016/0008-8846(73)90096-3.